

Range Correction for the CryoSat and GOCE Laser Retroreflector Arrays

O.Montenbruck (DLR/GSOC), R.Neubert (GFZ)

Introduction

The Institute of Precision Instruments Engineering (IPIE), Moscow, provides various types of laser retroreflector arrays (LRA) for Earth orbiting satellites. Among others, IPI has manufactured LRAs for the CryoSat-1/2 [1], GOCE [2] and Proba-2 [3] missions of the European Space Agency (ESA) as well as the GIOVE-A/B navigation satellites. For use in low Earth orbit (LEO), a common design with one nadir-looking prism and six side-looking prisms is employed (Fig. 1). However, a slightly larger tilt angle of the side-looking prisms is used for GOCE in comparison to CryoSat and Proba-2 to account for the much lower orbital altitude.

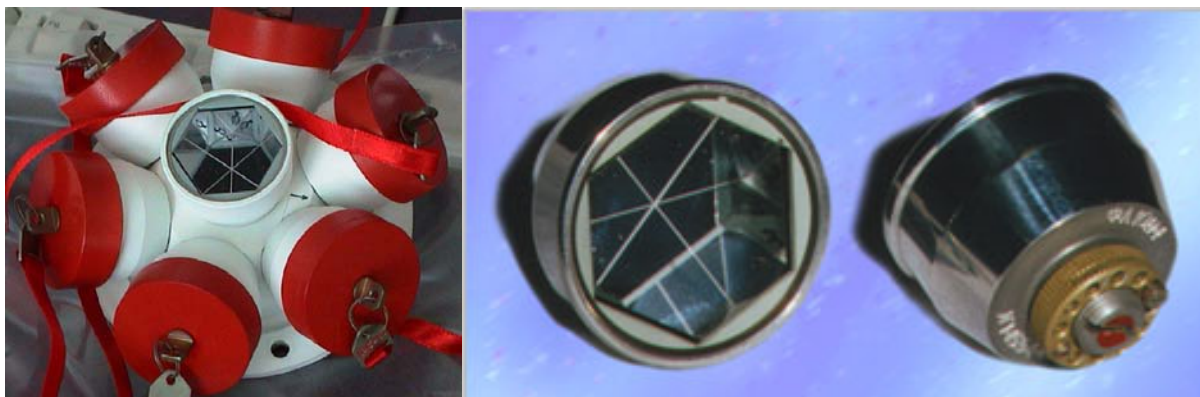


Fig. 1 IPIE laser retroreflector array for LEO satellites (left: GOCE flight model, right: individual prism). Images courtesy ESA and IPIE.

For the precision analysis of satellite laser ranging (SLR) measurements, a line-of-sight-dependent range correction must be considered. This correction describes the difference between the distance of the SLR station from a predefined LRA reference point and the actual range measurement. The range correction accounts for the path length within the prisms as well as the position of the prisms' input face centers with respect to the adopted reference point.

Elevation dependent range corrections for the two LRA types have been provided by IPIE in [2] and [3] and are, for example, adopted as processing standard for the validation of GOCE precise science orbit products ([4],[5]). However, a pronounced azimuth dependence must be expected from the LRA design and a one-dimensional correction function is obviously unsuitable for a proper modeling of SLR measurements. An effort is therefore made, to derive an azimuth-elevation dependent range correction for the GOCE and CryoSat/Proba-2 reflectors that will support an improved analysis of satellite laser tracking data for these missions. The analytical formulation of the range correction is based on previous work of Neubert [6] for the LRA of GeoForschungsZentrum (GFZ), Potsdam, but takes into account the specific geometry and parameters of the IPIE design.

LRA Parameters

Optical and mechanical parameters of the Type 1 (CryoSat-1/2, Proba-2) and Type 2 (GOCE) laser retroreflector arrays are summarized in Table 1 based on design information given in [1]-[3]. For illustration, design drawings of the reflectors are provided in Annex 1 (Figs. A1-A3). In accord with IPIE conventions, the center of the base plane is adopted as the mechanical reference point (MRP). It almost coincides with the optical reference point (ORP), which is defined by the intersection of the optical axes, for the Type 1 reflector array. For the Type 2 array, in contrast, the ORP is located at a distance of 6.8 mm from the MRP inside the LRA structure.

Table 1 Technical parameters of IPIE laser retroreflector arrays (derived from [1]-[3])

Parameter	Symbol	Type 1	Type 2
<i>Design values:</i>			
Number of reflectors		7	
Effective optical aperture of individual reflectors		$\varnothing 28.2$ mm	$\varnothing 28$ mm
Distance between prism surface and vertex	L	19.1 mm	
Height of input face center (central reflector)	h_0	48.0 mm	49.3 mm
Height of input face center (lateral reflectors)	$h_{1,\dots,6}$	28.5 mm	29.2 mm
Radial offset of input face center (lateral reflectors)	$s_{1,\dots,6}$	45.5 mm	48.0 mm
Tilt angle of lateral reflectors	ϕ	57.5°	65°
Mechanical reference point		Center of base plane	
<i>Derived quantities:</i>			
Optical reference point height		-0.49 mm	+6.82 mm
Distance of input face center from MRP (central reflector)		48.00 mm	49.30 mm
Distance of input face center from MRP (lateral reflectors)		53.69 mm	56.18 mm
Distance of input face center from ORP (central reflector)		48.49 mm	42.48 mm
Distance of input face center from ORP (lateral reflectors)		53.97 mm	52.96 mm

It may be recognized that the adopted tilt angles and positions cause a notable difference in the input face distance from the ORP (or MRP) for the central and lateral prisms. This difference causes a notable variation in the amplitude of the range correction and is most pronounced (roughly 10 mm) for the Type 2 reflector employed on GOCE.

For the computation of the range correction, a reference system is established, which originates in the center of the baseplane and is aligned with the principal axes of the LRA. The x/y-plane matches the baseplane and the z-axis coincides with the (nominally nadir-pointing) optical axis of the central prisms. The x-axis intersects two of the six lateral prisms, while the y-axis intersects two of the six mounting holes. In the absence of a unique numbering scheme for the individual prisms, we denote the central prism as #0. The lateral prisms are designated as #1,...,#6, starting at the +x prism and proceeding in a counterclockwise manner when looking in -z-direction. The resulting coordinates of the input face centers and the boresight direction are provided in Table 2.

Table 2 Location and orientation of the individual reflectors in the MRP centered LRA reference system

LRR #i	Location	Input face center	Optical axis
0	central	$r = \begin{pmatrix} 0 \\ 0 \\ h_0 \end{pmatrix}$	$n = \begin{pmatrix} 0 \\ 0 \\ 1 \end{pmatrix}$
1..6	lateral	$r = \begin{pmatrix} s_i \cdot \cos((i-1) \cdot \pi / 3) \\ s_i \cdot \sin((i-1) \cdot \pi / 3) \\ h_i \end{pmatrix}$	$n = \begin{pmatrix} \sin(\phi) \cdot \cos((i-1) \cdot \pi / 3) \\ \sin(\phi) \cdot \sin((i-1) \cdot \pi / 3) \\ \cos(\phi) \end{pmatrix}$

Range Correction

Following [6], the range correction for a single prism takes into account two contributions:

- The measured range is larger than the geometric distance of the input face center from the station by a contribution related to the light path inside the prism (taking into account the reduced group velocity in the refractive medium)
- The distance of the reference point and the input face center differ by an amount that equals the projection of the input face center position on the line-of-sight vector.

Defining the range correction $\Delta\rho$ as the difference of the measured range and the geometric distance of the reference point from the station¹, the following expression is obtained for the individual prisms ($i = 0, \dots, 6$):

$$\Delta\rho_i = \left[L\sqrt{n_g^2 + (\mathbf{e}^T \mathbf{n}_i)^2 - 1} \right] - [\mathbf{e}^T \mathbf{r}_i] \quad (1)$$

Here, L and n_g denote the vertex height and the group refractive index of the prism, \mathbf{e} is the line-of-sight unit vector (directed from the LRA to the station), \mathbf{n}_i is the optical axis unit vector (i.e. the vector perpendicular to the surface of the prism) and \mathbf{r}_i is the position of the input face center relative to the reference point. Eqn. (1) is generically valid for an arbitrary choice of the reference point (e.g. MRP or ORP) provided that the proper coordinates of the input face centers are used. Other than for the GFZ reflector, which exhibits a constant distance of the input face center from the ORP for all prisms, an ORP-related range correction does not provide specific advantages or simplifications. For ease of use and comparison with IPIE results, only the MRP-related range correction is considered in the sequel.

The effective range correction for a single photon detecting system working at low return rate is the weighted average

$$\Delta\rho = \left(\sum_{i=0}^6 S_i \cdot \Delta\rho_i \right) / \left(\sum_{i=0}^6 S_i \right) \quad (2)$$

of all contributing cube corner prisms. The weighting factors S_i depend on the location of the receiving station in the far field of the return beam. Because of manufacturing errors and thermal distortions the far field is not well known. Therefore we use the simple approximation

$$S_i(\mathbf{e}) = \left(1 - \frac{\arccos(\mathbf{e}^T \mathbf{n}_i)}{\gamma_{\max}} \right)^2 \quad (3)$$

for the weighting factors (see [6]). Here, γ_{\max} denotes the maximum off-boresight angle under which a reflection can be observed.

In the absence of more detailed information a group refractive index of $n_g = 1.4855$ (applicable for a quartz prism at a laser wavelength of 532 nm) and a limiting incidence angle of $\gamma_{\max} = 0.85$ rad are assumed in the subsequent analysis.

Alternatively, for strong signals the prism closest to the observer tends to dominate. Therefore we compute the range correction of the closest prism as an approximation of the strong signal case.

¹ Note that the range correction is defined as a (mostly positive) quantity that must be added to the observed range in the original work of Neubert as well as the IPIE documentation. Within the present report we prefer the alternative convention for compatibility with the treatment of GPS phase center corrections.

Range corrections obtained with the single- and multi-prism approximations are illustrated in Figs. 2 and 3 for the Type 1 and Type 2 reflectors, respectively. Here, elevation describes the angle between the LRA-to-station line-of-sight vector and the LRA ground plane (counted positive towards the nadir-pointing +z-axis). The azimuth angle measures the angle between the y-axis and the projection of the line-of-sight vector on the xy-plane. It is counted positive towards the x-axis. The convention follows established standards for the specification of GPS antenna phase patterns and a format adopted from the GPS ANTEX standard [7] is used for the range correction tables given in Annex 2.

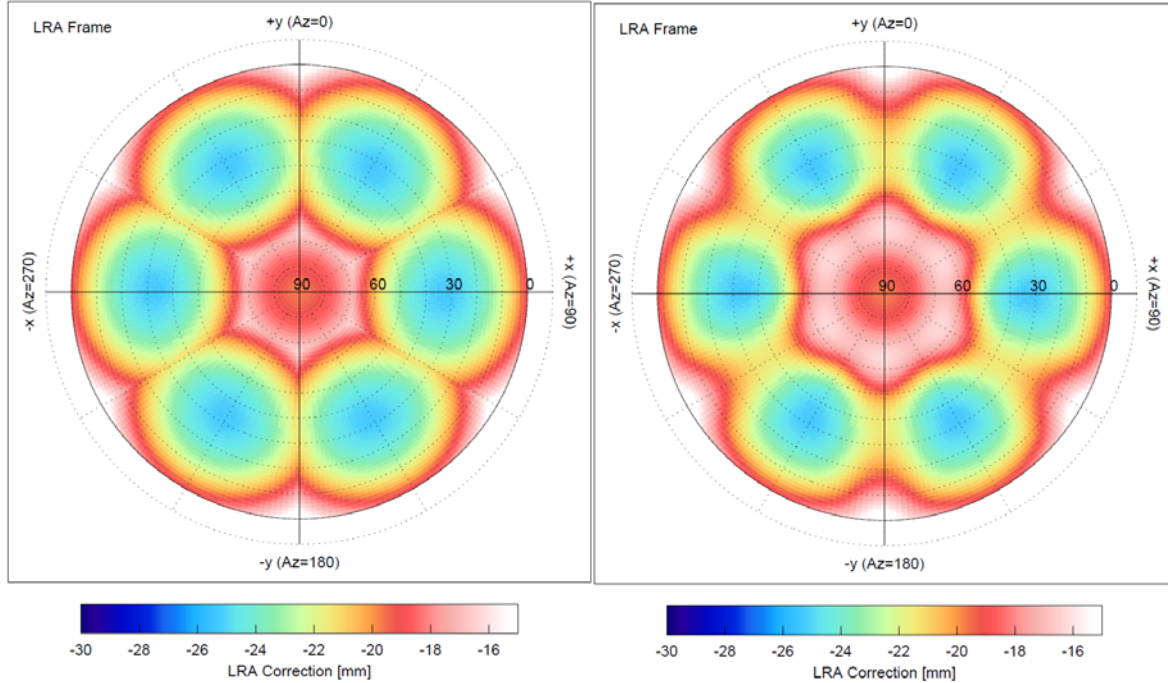


Fig. 2 Range correction of the IPIE Type 1 LRA of CryoSat as obtained from the nearest- (*left*) and multi-prism approximation (*right*).

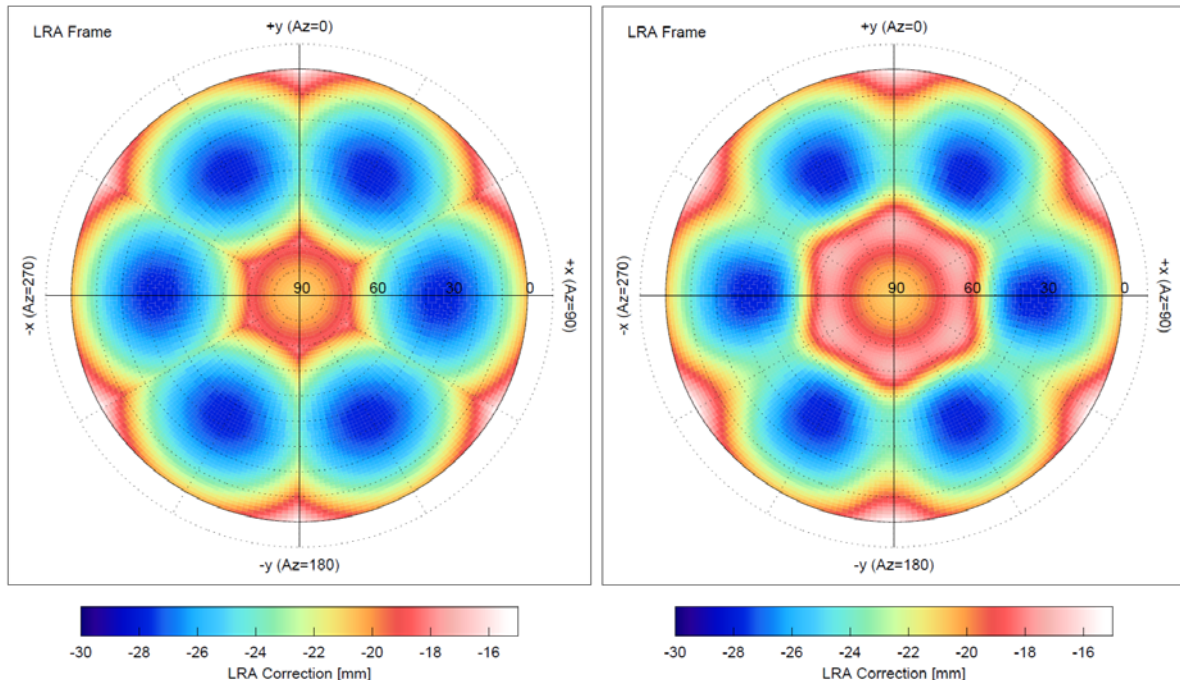


Fig. 3 Range correction of the IPIE Type 2 LRA of GOCE as obtained from the nearest- (*left*) and multi-prism approximation (*right*).

The elevation dependence of the range correction in the xz-plane (azimuth 0°) and the yz-plane (azimuth 90°) is furthermore illustrated in Figs. 4-5 for the two reflector types. While a purely elevation dependent function provides a good representation of the range correction for elevations above 60° , azimuth variations of about 5 mm are encountered below 40° elevation. At high elevations, the computed range correction shows a good agreement with IPIE values provided in [3] and [2]. However, major differences can be recognized at elevations of less than 70° .

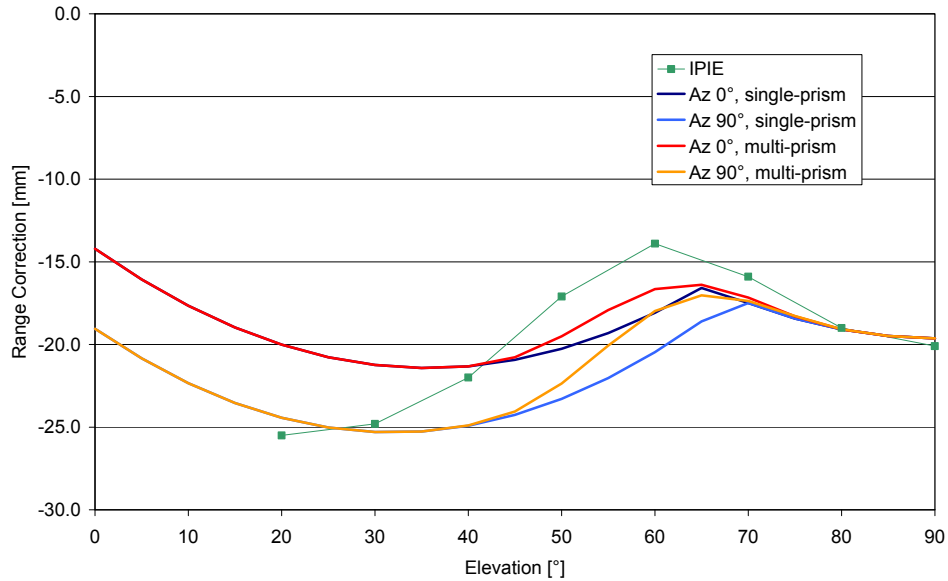


Fig. 4 Comparison of elevation dependent range corrections for IPIE Type 1 LRA of CryoSat.

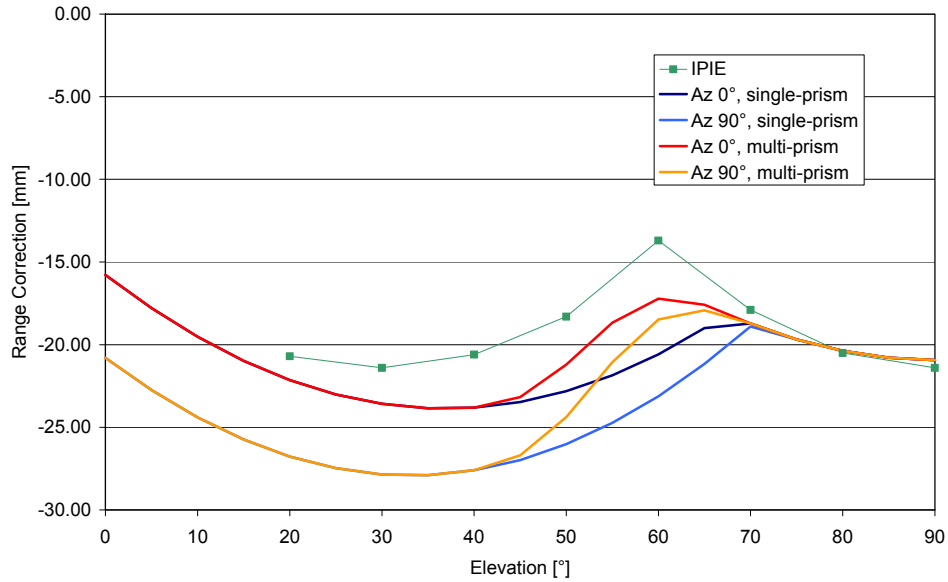


Fig. 5 Comparison of elevation dependent range corrections for IPIE Type 2 LRA of GOCE.

Summary and Conclusions

Azimuth- and elevation-dependent range corrections relative to the mechanical reference point have been computed for the IPIE laser retroreflector arrays of CryoSat and GOCE. The two reflector types use a similar design but differ in the tilt angle and placement of the side-looking prisms. As a consequence of the 7-prism design and a non-concentric arrangement of the central and lateral prisms, the range correction exhibits total variations of $\pm 5 \dots \pm 7$ mm about the mean value. A purely elevation-dependent correction appears unsuitable for a precision modeling of satellite laser ranging measurements and provides only moderate advantages over a constant range bias. Range corrections computed within the present study exhibit notable (~ 5 mm) differences with respect to range corrections provided by the manufacturer at elevations of less than 60° , while a good agreement is obtained close to the nadir direction. Further efforts will be required to independently validate the proposed range corrections through actual laser ranging measurements of CryoSat and GOCE.

References

- [1] Shargorodsky V.; "CryoSat-LRR-01 Laser Retro Reflector Technical Description"; Doc. No. K01-Э095-00-00 TO; Scientific Research Institute for Precision Instruments, Moscow, 2002.
URL http://ilrs.gsfc.nasa.gov/docs/CRYOSAT_LRR_01_DATA_PACKAGE.pdf; last acc. 24 June 2011
- [2] Shargorodsky V.; "GOCE-LRR Laser Retro Reflector Technical Description"; Doc. No. K01-Э095-00-00 TO; Scientific Research Institute for Precision Instruments, Moscow, 2004.
URL <http://ilrs.gsfc.nasa.gov/docs/GOCE-LRR-01SetofDocuments.pdf>; last accessed 24 June 2011.
- [3] Shargorodsky V.; "Technical Description of the Laser Retroreflector array PROBA-2-LRR-01"; Doc. No. K01-Э285-00-00 TO; Institute for Precision Instruments Engineering, Moscow, 2007.
- [4] Bock H., Jäggi A.; "GOCE SSTI antenna and LRR positions"; GO-TN-HPF-GS-0269; Issue 1.0, 26.01.2010; European GOCE Gravity Consortium (2010).
- [5] Bigazzi A., Frommknecht B.; "Note on GOCE Instrument Positioning"; XGCE-GSEG-EOPG-TN-09-0007, Issue 3.1, 1 Mar. 2010; ESA (2010).
- [6] Neubert R.; "The Center of Mass Correction (CoM) for Laser Ranging Data of the CHAMP Reflector"; Issue C, 14 Oct 2009. URL http://ilrs.gsfc.nasa.gov/docs/CH_GRACE_COM_c.pdf, acc. 2 Nov 2009.
- [7] Rothacher M., Schmid R.; „ANTEX: The Antenna Exchange Format, Version 1.4“ Forschungseinrichtung Satellitengeodäsie, TU München, 15 Sep. 2010.
URL <http://igscb.jpl.nasa.gov/igscb/station/general/antex14.txt>; last accessed 24 June 2011.

Annex 1 – Design Drawings

Design drawings of the Cryosat-1/2, PROBA-2 and GOCE laser retroreflector arrays are given in Figs. A1-A3.

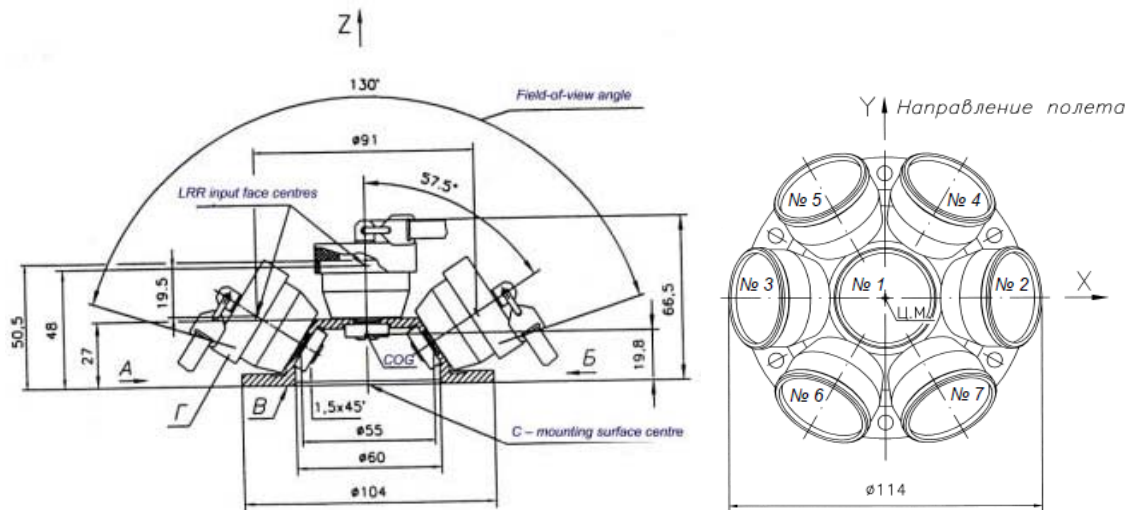


Fig .A1 CryoSat-1/2 laser retroreflector array (from [1])

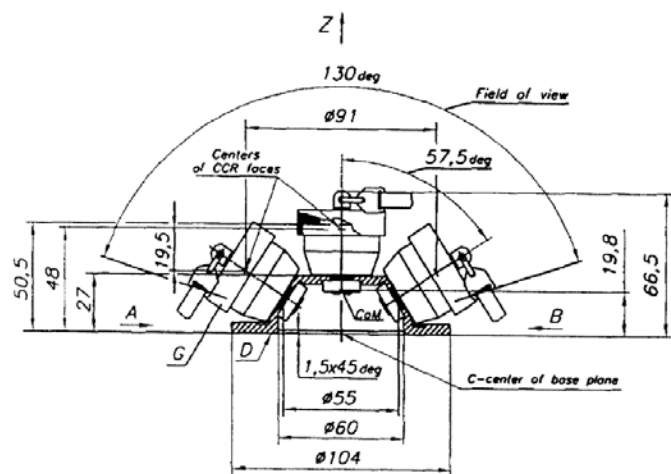


Fig. A2 Proba-2 laser retroreflector array (from [3])

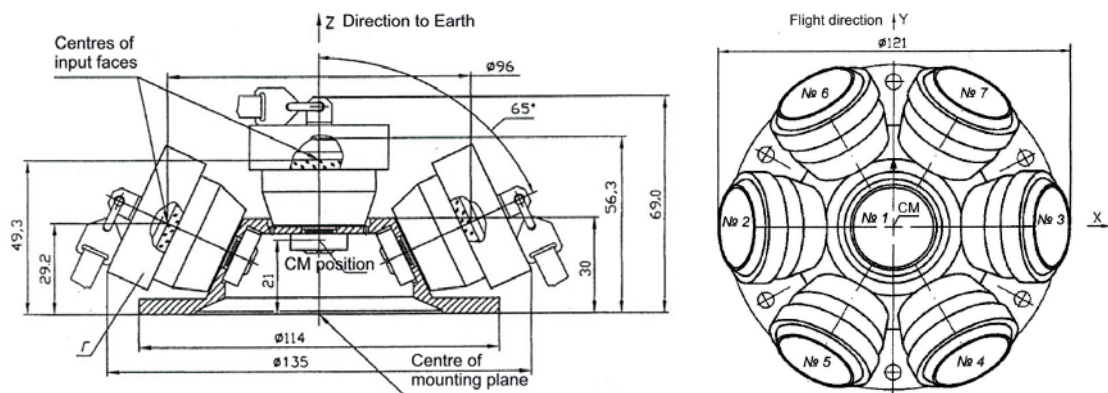


Fig. A3 GOCE laser retroreflector array (from [2])

Annex 2 – Range Corrections

Range corrections for the various reflector types in single- and multi-prism approximation are provided below. The format of the range correction files is adopted from the ANTEX standard employed for GPS antenna phase patterns [7]. Due to the rotational symmetry of the LRA design, only a subset of azimuth values is given in the printouts.

Type 1 LRA – Nearest-Prism Approximation

```

1.0                                     LRAEX VERSION
                                         COMMENT
Ranging correction for IPIE laser retroreflector assembly   COMMENT
of CRYO based on nearest-prism solution                      COMMENT
as a function of azimuth and boresight (nadir) angle        COMMENT
                                         COMMENT
Must be added to modeled range of optical reference point. COMMENT
                                         COMMENT
                                         COMMENT
                                         END OF HEADER
                                         START OF LRA
IPIECRYO                               TYPE / SERIAL NO
5.0                                     DAZI
0.0 90.0 5.0                           ZEN1 / ZEN2 / DZEN
532.0                                     WAVELENGTH
0.0 -19.63 -19.49 -19.09 -18.43 -17.49 -16.58 -18.08 -19.31 -20.26 -20.93 -21.32 -21.42 -21.24 -20.77 -20.01 -18.97 -17.66 -16.07 -14.21
5.0 -19.63 -19.49 -19.09 -18.43 -17.49 -17.19 -18.80 -20.13 -21.18 -21.94 -22.41 -22.58 -22.46 -22.05 -21.35 -20.36 -19.08 -17.51 -15.68
10.0 -19.63 -19.49 -19.09 -18.43 -17.49 -17.70 -19.39 -20.81 -21.93 -22.77 -23.30 -23.54 -23.48 -23.11 -22.45 -21.50 -20.25 -18.71 -16.88
15.0 -19.63 -19.49 -19.09 -18.43 -17.49 -18.09 -19.86 -21.34 -22.53 -23.42 -24.00 -24.29 -24.27 -23.94 -23.32 -22.39 -21.16 -19.64 -17.83
20.0 -19.63 -19.49 -19.09 -18.43 -17.49 -18.38 -20.20 -21.72 -22.95 -23.88 -24.51 -24.83 -24.84 -24.54 -23.94 -23.03 -21.82 -20.31 -18.50
25.0 -19.63 -19.49 -19.09 -18.43 -17.49 -18.55 -20.40 -21.95 -23.21 -24.16 -24.81 -25.15 -25.18 -24.90 -24.31 -23.41 -22.21 -20.71 -18.91
30.0 -19.63 -19.49 -19.09 -18.43 -17.49 -18.61 -20.46 -22.03 -23.29 -24.26 -24.91 -25.26 -25.29 -25.02 -24.43 -23.54 -22.34 -20.84 -19.05
35.0 -19.63 -19.49 -19.09 -18.43 -17.49 -18.55 -20.40 -21.95 -23.21 -24.16 -24.81 -25.15 -25.18 -24.90 -24.31 -23.41 -22.21 -20.71 -18.91
40.0 -19.63 -19.49 -19.09 -18.43 -17.49 -18.38 -20.20 -21.72 -22.95 -23.88 -24.51 -24.83 -24.84 -24.54 -23.94 -23.03 -21.82 -20.31 -18.50
45.0 -19.63 -19.49 -19.09 -18.43 -17.49 -18.09 -19.86 -21.34 -22.53 -23.42 -24.00 -24.29 -24.27 -23.94 -23.32 -22.39 -21.16 -19.64 -17.83
50.0 -19.63 -19.49 -19.09 -18.43 -17.49 -17.70 -19.39 -20.81 -21.93 -22.77 -23.30 -23.54 -23.48 -23.11 -22.45 -21.50 -20.25 -18.71 -16.88
55.0 -19.63 -19.49 -19.09 -18.43 -17.49 -17.19 -18.80 -20.13 -21.18 -21.94 -22.41 -22.58 -22.46 -22.05 -21.35 -20.36 -19.08 -17.51 -15.68
60.0 -19.63 -19.49 -19.09 -18.43 -17.49 -16.58 -18.08 -19.31 -20.26 -20.93 -21.32 -21.42 -21.24 -20.77 -20.01 -18.97 -17.66 -16.07 -14.21
...
300.0 -19.63 -19.49 -19.09 -18.43 -17.49 -16.58 -18.08 -19.31 -20.26 -20.93 -21.32 -21.42 -21.24 -20.77 -20.01 -18.97 -17.66 -16.07 -14.21
305.0 -19.63 -19.49 -19.09 -18.43 -17.49 -17.19 -18.80 -20.13 -21.18 -21.94 -22.41 -22.58 -22.46 -22.05 -21.35 -20.36 -19.08 -17.51 -15.68
310.0 -19.63 -19.49 -19.09 -18.43 -17.49 -17.70 -19.39 -20.81 -21.93 -22.77 -23.30 -23.54 -23.48 -23.11 -22.45 -21.50 -20.25 -18.71 -16.88
315.0 -19.63 -19.49 -19.09 -18.43 -17.49 -18.09 -19.86 -21.34 -22.53 -23.42 -24.00 -24.29 -24.27 -23.94 -23.32 -22.39 -21.16 -19.64 -17.83
320.0 -19.63 -19.49 -19.09 -18.43 -17.49 -18.38 -20.20 -21.72 -22.95 -23.88 -24.51 -24.83 -24.84 -24.54 -23.94 -23.03 -21.82 -20.31 -18.50
325.0 -19.63 -19.49 -19.09 -18.43 -17.49 -18.55 -20.40 -21.95 -23.21 -24.16 -24.81 -25.15 -25.18 -24.90 -24.31 -23.41 -22.21 -20.71 -18.91
330.0 -19.63 -19.49 -19.09 -18.43 -17.49 -18.61 -20.46 -22.03 -23.29 -24.26 -24.91 -25.26 -25.29 -25.02 -24.43 -23.54 -22.34 -20.84 -19.05
335.0 -19.63 -19.49 -19.09 -18.43 -17.49 -18.55 -20.40 -21.95 -23.21 -24.16 -24.81 -25.15 -25.18 -24.90 -24.31 -23.41 -22.21 -20.71 -18.91
340.0 -19.63 -19.49 -19.09 -18.43 -17.49 -18.38 -20.20 -21.72 -22.95 -23.88 -24.51 -24.83 -24.84 -24.54 -23.94 -23.03 -21.82 -20.31 -18.50
345.0 -19.63 -19.49 -19.09 -18.43 -17.49 -18.09 -19.86 -21.34 -22.53 -23.42 -24.00 -24.29 -24.27 -23.94 -23.32 -22.39 -21.16 -19.64 -17.83
350.0 -19.63 -19.49 -19.09 -18.43 -17.49 -17.70 -19.39 -20.81 -21.93 -22.77 -23.30 -23.54 -23.48 -23.11 -22.45 -21.50 -20.25 -18.71 -16.88
355.0 -19.63 -19.49 -19.09 -18.43 -17.49 -17.19 -18.80 -20.13 -21.18 -21.94 -22.41 -22.58 -22.46 -22.05 -21.35 -20.36 -19.08 -17.51 -15.68
360.0 -19.63 -19.49 -19.09 -18.43 -17.49 -16.58 -18.08 -19.31 -20.26 -20.93 -21.32 -21.42 -21.24 -20.77 -20.01 -18.97 -17.66 -16.07 -14.21
                                         END OF LRA

```

Type 1 LRA – Multi-Prism Approximation

```

1.0                                     LRAEX VERSION
                                         COMMENT
Ranging correction for IPIE laser retroreflector assembly   COMMENT
of CRYO based on single-prism solution                      COMMENT
as a function of azimuth and boresight (nadir) angle        COMMENT
                                         COMMENT
Must be added to modeled range of optical reference point. COMMENT
                                         COMMENT
                                         COMMENT
                                         END OF HEADER
                                         START OF LRA
                                         TYPE / SERIAL NO
IPIECRYO
5.0
0.0 90.0 5.0
532.0
                                         ZEN1 / ZEN2 / DZEN
                                         WAVELENGTH
      0.0 -19.63 -19.49 -19.09 -18.29 -17.16 -16.39 -16.65 -17.92 -19.51 -20.77 -21.32 -21.42 -21.24 -20.77 -20.01 -18.97 -17.66 -16.07 -14.21
      5.0 -19.63 -19.49 -19.09 -18.29 -17.17 -16.43 -16.73 -18.05 -19.70 -21.01 -21.60 -21.74 -21.60 -21.18 -20.48 -19.52 -18.32 -16.93 -15.44
     10.0 -19.63 -19.49 -19.09 -18.29 -17.21 -16.53 -16.95 -18.41 -20.20 -21.63 -22.32 -22.57 -22.53 -22.21 -21.63 -20.81 -19.79 -18.56 -16.88
     15.0 -19.63 -19.49 -19.09 -18.29 -17.26 -16.68 -17.26 -18.92 -20.89 -22.44 -23.24 -23.59 -23.64 -23.40 -22.90 -22.15 -21.11 -19.64 -17.83
     20.0 -19.63 -19.49 -19.09 -18.29 -17.31 -16.84 -17.58 -19.44 -21.57 -23.22 -24.08 -24.49 -24.58 -24.37 -23.87 -23.03 -21.82 -20.31 -18.50
     25.0 -19.63 -19.49 -19.09 -18.28 -17.35 -16.97 -17.86 -19.87 -22.11 -23.81 -24.67 -25.07 -25.15 -24.90 -24.31 -23.41 -22.21 -20.71 -18.91
     30.0 -19.63 -19.49 -19.08 -18.28 -17.36 -17.03 -17.98 -20.07 -22.36 -24.06 -24.90 -25.26 -25.29 -25.02 -24.43 -23.54 -22.34 -20.84 -19.05
     35.0 -19.63 -19.49 -19.09 -18.28 -17.35 -16.97 -17.86 -19.87 -22.11 -23.81 -24.67 -25.07 -25.15 -24.90 -24.31 -23.41 -22.21 -20.71 -18.91
     40.0 -19.63 -19.49 -19.09 -18.29 -17.31 -16.84 -17.58 -19.44 -21.57 -23.22 -24.08 -24.49 -24.58 -24.37 -23.87 -23.03 -21.82 -20.31 -18.50
     45.0 -19.63 -19.49 -19.09 -18.29 -17.26 -16.68 -17.26 -18.92 -20.89 -22.44 -23.24 -23.59 -23.64 -23.40 -22.90 -22.15 -21.11 -19.64 -17.83
     50.0 -19.63 -19.49 -19.09 -18.29 -17.21 -16.53 -16.95 -18.41 -20.20 -21.63 -22.32 -22.57 -22.53 -22.21 -21.63 -20.81 -19.79 -18.56 -16.88
     55.0 -19.63 -19.49 -19.09 -18.29 -17.17 -16.43 -16.73 -18.05 -19.70 -21.01 -21.60 -21.74 -21.60 -21.18 -20.48 -19.52 -18.32 -16.93 -15.44
     60.0 -19.63 -19.49 -19.09 -18.29 -17.16 -16.39 -16.65 -17.92 -19.51 -20.77 -21.32 -21.42 -21.24 -20.77 -20.01 -18.97 -17.66 -16.07 -14.21
...
      300.0 -19.63 -19.49 -19.09 -18.29 -17.16 -16.39 -16.65 -17.92 -19.51 -20.77 -21.32 -21.42 -21.24 -20.77 -20.01 -18.97 -17.66 -16.07 -14.21
      305.0 -19.63 -19.49 -19.09 -18.29 -17.17 -16.43 -16.73 -18.05 -19.70 -21.01 -21.60 -21.74 -21.60 -21.18 -20.48 -19.52 -18.32 -16.93 -15.44
      310.0 -19.63 -19.49 -19.09 -18.29 -17.21 -16.53 -16.95 -18.41 -20.20 -21.63 -22.32 -22.57 -22.53 -22.21 -21.63 -20.81 -19.79 -18.56 -16.88
      315.0 -19.63 -19.49 -19.09 -18.29 -17.26 -16.68 -17.26 -18.92 -20.89 -22.44 -23.24 -23.59 -23.64 -23.40 -22.90 -22.15 -21.11 -19.64 -17.83
      320.0 -19.63 -19.49 -19.09 -18.29 -17.31 -16.84 -17.58 -19.44 -21.57 -23.22 -24.08 -24.49 -24.58 -24.37 -23.87 -23.03 -21.82 -20.31 -18.50
      325.0 -19.63 -19.49 -19.09 -18.28 -17.35 -16.97 -17.86 -19.87 -22.11 -23.81 -24.67 -25.07 -25.15 -24.90 -24.31 -23.41 -22.21 -20.71 -18.91
      330.0 -19.63 -19.49 -19.08 -18.28 -17.36 -17.03 -17.98 -20.07 -22.36 -24.06 -24.90 -25.26 -25.29 -25.02 -24.43 -23.54 -22.34 -20.84 -19.05
      335.0 -19.63 -19.49 -19.09 -18.28 -17.35 -16.97 -17.86 -19.87 -22.11 -23.81 -24.67 -25.07 -25.15 -24.90 -24.31 -23.41 -22.21 -20.71 -18.91
      340.0 -19.63 -19.49 -19.09 -18.29 -17.31 -16.84 -17.58 -19.44 -21.57 -23.22 -24.08 -24.49 -24.58 -24.37 -23.87 -23.03 -21.82 -20.31 -18.50
      345.0 -19.63 -19.49 -19.09 -18.29 -17.26 -16.68 -17.26 -18.92 -20.89 -22.44 -23.24 -23.59 -23.64 -23.40 -22.90 -22.15 -21.11 -19.64 -17.83
      350.0 -19.63 -19.49 -19.09 -18.29 -17.21 -16.53 -16.95 -18.41 -20.20 -21.63 -22.32 -22.57 -22.53 -22.21 -21.63 -20.81 -19.79 -18.56 -16.88
      355.0 -19.63 -19.49 -19.09 -18.29 -17.17 -16.43 -16.73 -18.05 -19.70 -21.01 -21.60 -21.74 -21.60 -21.18 -20.48 -19.52 -18.32 -16.93 -15.44
      360.0 -19.63 -19.49 -19.09 -18.29 -17.16 -16.39 -16.65 -17.92 -19.51 -20.77 -21.32 -21.42 -21.24 -20.77 -20.01 -18.97 -17.66 -16.07 -14.21
                                         END OF LRA

```

Type 2 LRA – Nearest-Prism Approximation

1.0

LRAEX VERSION

Ranging correction for IPIE laser retroreflector assembly COMMENT

of GOCE based on nearest-prism solution COMMENT

as a function of azimuth and boresight (nadir) angle COMMENT

Must be added to modeled range of optical reference point. COMMENT

COMMENT

COMMENT

COMMENT

END OF HEADER

START OF LRA

TYPE / SERIAL NO

IPIEGOCE

	DAZI	ZEN1 / ZEN2 / DZEN	WAVELENGTH																	
5.0	0.0	90.0	5.0																	
532.0	0.0	-20.93	-20.79	-20.37	-19.68	-18.72	-19.00	-20.58	-21.85	-22.81	-23.47	-23.81	-23.85	-23.58	-23.01	-22.14	-20.98	-19.52	-17.79	-15.78
5.0	-20.93	-20.79	-20.37	-19.68	-18.72	-19.66	-21.34	-22.72	-23.78	-24.53	-24.96	-25.07	-24.87	-24.36	-23.54	-22.42	-21.00	-19.29	-17.30	
10.0	-20.93	-20.79	-20.37	-19.68	-18.72	-20.20	-21.98	-23.44	-24.58	-25.41	-25.90	-26.08	-25.94	-25.47	-24.70	-23.61	-22.22	-20.53	-18.56	
15.0	-20.93	-20.79	-20.37	-19.68	-18.72	-20.62	-22.47	-24.00	-25.21	-26.09	-26.64	-26.87	-26.77	-26.34	-25.60	-24.54	-23.17	-21.50	-19.54	
20.0	-20.93	-20.79	-20.37	-19.68	-18.72	-20.93	-22.83	-24.41	-25.66	-26.58	-27.17	-27.44	-27.37	-26.97	-26.25	-25.21	-23.85	-22.19	-20.24	
25.0	-20.93	-20.79	-20.37	-19.68	-18.85	-21.11	-23.04	-24.65	-25.93	-26.88	-27.49	-27.78	-27.73	-27.34	-26.64	-25.61	-24.27	-22.61	-20.66	
30.0	-20.93	-20.79	-20.37	-19.68	-18.90	-21.17	-23.12	-24.73	-26.02	-26.98	-27.60	-27.89	-27.85	-27.47	-26.77	-25.74	-24.40	-22.75	-20.80	
35.0	-20.93	-20.79	-20.37	-19.68	-18.85	-21.11	-23.04	-24.65	-25.93	-26.88	-27.49	-27.78	-27.73	-27.34	-26.64	-25.61	-24.27	-22.61	-20.66	
40.0	-20.93	-20.79	-20.37	-19.68	-18.72	-20.93	-22.83	-24.41	-25.66	-26.58	-27.17	-27.44	-27.37	-26.97	-26.25	-25.21	-23.85	-22.19	-20.24	
45.0	-20.93	-20.79	-20.37	-19.68	-18.72	-20.62	-22.47	-24.00	-25.21	-26.09	-26.64	-26.87	-26.77	-26.34	-25.60	-24.54	-23.17	-21.50	-19.54	
50.0	-20.93	-20.79	-20.37	-19.68	-18.72	-20.20	-21.98	-23.44	-24.58	-25.41	-25.90	-26.08	-25.94	-25.47	-24.70	-23.61	-22.22	-20.53	-18.56	
55.0	-20.93	-20.79	-20.37	-19.68	-18.72	-19.66	-21.34	-22.72	-23.78	-24.53	-24.96	-25.07	-24.87	-24.36	-23.54	-22.42	-21.00	-19.29	-17.30	
60.0	-20.93	-20.79	-20.37	-19.68	-18.72	-19.00	-20.58	-21.85	-22.81	-23.47	-23.81	-23.85	-23.58	-23.01	-22.14	-20.98	-19.52	-17.79	-15.78	
...																				
300.0	-20.93	-20.79	-20.37	-19.68	-18.72	-19.00	-20.58	-21.85	-22.81	-23.47	-23.81	-23.85	-23.58	-23.01	-22.14	-20.98	-19.52	-17.79	-15.78	
305.0	-20.93	-20.79	-20.37	-19.68	-18.72	-19.66	-21.34	-22.72	-23.78	-24.53	-24.96	-25.07	-24.87	-24.36	-23.54	-22.42	-21.00	-19.29	-17.30	
310.0	-20.93	-20.79	-20.37	-19.68	-18.72	-20.20	-21.98	-23.44	-24.58	-25.41	-25.90	-26.08	-25.94	-25.47	-24.70	-23.61	-22.22	-20.53	-18.56	
315.0	-20.93	-20.79	-20.37	-19.68	-18.72	-20.62	-22.47	-24.00	-25.21	-26.09	-26.64	-26.87	-26.77	-26.34	-25.60	-24.54	-23.17	-21.50	-19.54	
320.0	-20.93	-20.79	-20.37	-19.68	-18.72	-20.93	-22.83	-24.41	-25.66	-26.58	-27.17	-27.44	-27.37	-26.97	-26.25	-25.21	-23.85	-22.19	-20.24	
325.0	-20.93	-20.79	-20.37	-19.68	-18.85	-21.11	-23.04	-24.65	-25.93	-26.88	-27.49	-27.78	-27.73	-27.34	-26.64	-25.61	-24.27	-22.61	-20.66	
330.0	-20.93	-20.79	-20.37	-19.68	-18.90	-21.17	-23.12	-24.73	-26.02	-26.98	-27.60	-27.89	-27.85	-27.47	-26.77	-25.74	-24.40	-22.75	-20.80	
335.0	-20.93	-20.79	-20.37	-19.68	-18.85	-21.11	-23.04	-24.65	-25.93	-26.88	-27.49	-27.78	-27.73	-27.34	-26.64	-25.61	-24.27	-22.61	-20.66	
340.0	-20.93	-20.79	-20.37	-19.68	-18.72	-20.93	-22.83	-24.41	-25.66	-26.58	-27.17	-27.44	-27.37	-26.97	-26.25	-25.21	-23.85	-22.19	-20.24	
345.0	-20.93	-20.79	-20.37	-19.68	-18.72	-20.62	-22.47	-24.00	-25.21	-26.09	-26.64	-26.87	-26.77	-26.34	-25.60	-24.54	-23.17	-21.50	-19.54	
350.0	-20.93	-20.79	-20.37	-19.68	-18.72	-20.20	-21.98	-23.44	-24.58	-25.41	-25.90	-26.08	-25.94	-25.47	-24.70	-23.61	-22.22	-20.53	-18.56	
355.0	-20.93	-20.79	-20.37	-19.68	-18.72	-19.66	-21.34	-22.72	-23.78	-24.53	-24.96	-25.07	-24.87	-24.36	-23.54	-22.42	-21.00	-19.29	-17.30	
360.0	-20.93	-20.79	-20.37	-19.68	-18.72	-19.00	-20.58	-21.85	-22.81	-23.47	-23.81	-23.85	-23.58	-23.01	-22.14	-20.98	-19.52	-17.79	-15.78	

END OF LRA

Type 2 LRA – Multi-Prism Approximation

```

1.0                                         LRAEX VERSION
                                         COMMENT
Ranging correction for IPIE laser retroreflector assembly   COMMENT
of GOCE based on multi-prism solution                      COMMENT
as a function of azimuth and boresight (nadir) angle       COMMENT
                                         COMMENT
Must be added to modeled range of optical reference point. COMMENT
                                         COMMENT
                                         COMMENT
                                         END OF HEADER
                                         START OF LRA
                                         TYPE / SERIAL NO
IPIEGOCE
5.0
0.0 90.0 5.0
532.0
0.0 -20.93 -20.79 -20.37 -19.68 -18.72 -17.58 -17.22 -18.67 -21.21 -23.17 -23.81 -23.58 -23.01 -22.14 -20.98 -19.52 -17.79 -15.78
5.0 -20.93 -20.79 -20.37 -19.68 -18.71 -17.60 -17.31 -18.86 -21.48 -23.47 -24.16 -24.23 -24.01 -23.48 -22.66 -21.54 -20.16 -18.53 -16.69
10.0 -20.93 -20.79 -20.37 -19.68 -18.71 -17.68 -17.57 -19.36 -22.16 -24.26 -25.03 -25.19 -25.06 -24.63 -23.89 -22.88 -21.61 -20.12 -18.40
15.0 -20.93 -20.79 -20.37 -19.68 -18.71 -17.77 -17.91 -20.01 -23.03 -25.24 -26.08 -26.32 -26.27 -25.90 -25.23 -24.27 -23.02 -21.48 -19.54
20.0 -20.93 -20.79 -20.37 -19.68 -18.72 -17.85 -18.21 -20.60 -23.81 -26.09 -26.97 -27.25 -27.22 -26.87 -26.20 -25.20 -23.85 -22.19 -20.24
25.0 -20.93 -20.79 -20.37 -19.68 -18.72 -17.90 -18.41 -20.95 -24.26 -26.59 -27.49 -27.77 -27.73 -27.34 -26.64 -25.61 -24.27 -22.61 -20.66
30.0 -20.93 -20.79 -20.37 -19.68 -18.72 -17.92 -18.47 -21.06 -24.38 -26.70 -27.60 -27.89 -27.85 -27.47 -26.77 -25.74 -24.40 -22.75 -20.80
35.0 -20.93 -20.79 -20.37 -19.68 -18.72 -17.90 -18.41 -20.95 -24.26 -26.59 -27.49 -27.77 -27.73 -27.34 -26.64 -25.61 -24.27 -22.61 -20.66
40.0 -20.93 -20.79 -20.37 -19.68 -18.72 -17.85 -18.21 -20.60 -23.81 -26.09 -26.97 -27.25 -27.22 -26.87 -26.20 -25.20 -23.85 -22.19 -20.24
45.0 -20.93 -20.79 -20.37 -19.68 -18.71 -17.77 -17.91 -20.01 -23.03 -25.24 -26.08 -26.32 -26.27 -25.90 -25.23 -24.27 -23.02 -21.48 -19.54
50.0 -20.93 -20.79 -20.37 -19.68 -18.71 -17.68 -17.57 -19.36 -22.16 -24.26 -25.03 -25.19 -25.06 -24.63 -23.89 -22.88 -21.61 -20.12 -18.40
55.0 -20.93 -20.79 -20.37 -19.68 -18.71 -17.60 -17.31 -18.86 -21.48 -23.47 -24.16 -24.23 -24.01 -23.48 -22.66 -21.54 -20.16 -18.53 -16.69
60.0 -20.93 -20.79 -20.37 -19.68 -18.72 -17.58 -17.22 -18.67 -21.21 -23.17 -23.81 -23.58 -23.01 -22.14 -20.98 -19.52 -17.79 -15.78

...
300.0 -20.93 -20.79 -20.37 -19.68 -18.72 -17.58 -17.22 -18.67 -21.21 -23.17 -23.81 -23.58 -23.01 -22.14 -20.98 -19.52 -17.79 -15.78
305.0 -20.93 -20.79 -20.37 -19.68 -18.71 -17.60 -17.31 -18.86 -21.48 -23.47 -24.16 -24.23 -24.01 -23.48 -22.66 -21.54 -20.16 -18.53 -16.69
310.0 -20.93 -20.79 -20.37 -19.68 -18.71 -17.68 -17.57 -19.36 -22.16 -24.26 -25.03 -25.19 -25.06 -24.63 -23.89 -22.88 -21.61 -20.12 -18.40
315.0 -20.93 -20.79 -20.37 -19.68 -18.71 -17.77 -17.91 -20.01 -23.03 -25.24 -26.08 -26.32 -26.27 -25.90 -25.23 -24.27 -23.02 -21.48 -19.54
320.0 -20.93 -20.79 -20.37 -19.68 -18.72 -17.85 -18.21 -20.60 -23.81 -26.09 -26.97 -27.25 -27.22 -26.87 -26.20 -25.20 -23.85 -22.19 -20.24
325.0 -20.93 -20.79 -20.37 -19.68 -18.72 -17.90 -18.41 -20.95 -24.26 -26.59 -27.49 -27.77 -27.73 -27.34 -26.64 -25.61 -24.27 -22.61 -20.66
330.0 -20.93 -20.79 -20.37 -19.68 -18.72 -17.92 -18.47 -21.06 -24.38 -26.70 -27.60 -27.89 -27.85 -27.47 -26.77 -25.74 -24.40 -22.75 -20.80
335.0 -20.93 -20.79 -20.37 -19.68 -18.72 -17.90 -18.41 -20.95 -24.26 -26.59 -27.49 -27.77 -27.73 -27.34 -26.64 -25.61 -24.27 -22.61 -20.66
340.0 -20.93 -20.79 -20.37 -19.68 -18.72 -17.85 -18.21 -20.60 -23.81 -26.09 -26.97 -27.25 -27.22 -26.87 -26.20 -25.20 -23.85 -22.19 -20.24
345.0 -20.93 -20.79 -20.37 -19.68 -18.71 -17.77 -17.91 -20.01 -23.03 -25.24 -26.08 -26.32 -26.27 -25.90 -25.23 -24.27 -23.02 -21.48 -19.54
350.0 -20.93 -20.79 -20.37 -19.68 -18.71 -17.68 -17.57 -19.36 -22.16 -24.26 -25.03 -25.19 -25.06 -24.63 -23.89 -22.88 -21.61 -20.12 -18.40
355.0 -20.93 -20.79 -20.37 -19.68 -18.71 -17.60 -17.31 -18.86 -21.48 -23.47 -24.16 -24.23 -24.01 -23.48 -22.66 -21.54 -20.16 -18.53 -16.69
360.0 -20.93 -20.79 -20.37 -19.68 -18.72 -17.58 -17.22 -18.67 -21.21 -23.17 -23.81 -23.58 -23.01 -22.14 -20.98 -19.52 -17.79 -15.78

                                         END OF LRA

```